DOI: 10.1002/ejic.200600377

Encouraging Chromium(III) Ions to Form Larger Clusters: Syntheses, Structures, Magnetic Properties and Theoretical Studies of Di- and Octametallic Cr Clusters

Caytie E. Talbot-Eeckelaers,[a] Gopalan Rajaraman,[a] Joan Cano,*[b,c,d] Guillem Aromí,[b] Eliseo Ruiz,[b,c] and Euan K. Brechin*[a,e]

Keywords: Exchange coupling / Density functional theory / Polynuclear chromium complexes / Magnetic properties / Magneto-structural correlation

Reaction of anhydrous $CrCl_2$ with the tripodal ligands 1,1,1-tris(hydroxymethyl)ethane (H_3thme), 1,1,1-tris(hydroxymethyl)propane (H_3tmp) and pentaerythritol (H_4peol) produces three new Cr^{III} clusters that have been structurally and magnetically characterised. The dimeric complex $[Cr_2(H_2tmp)_2Cl_4]\cdot 2MeOH$ (**1**·2MeOH) is generated under reflux. An analogous reaction, but under solvothermal conditions produces the octametallic species $[Cr_8O_2(thme)_2(Hthme)_4Cl_6]\cdot 2MeOH$ (**2**·2MeOH) and $[Cr_8O_2(Hpeol)_2(H_2peol)_4Cl_6]\cdot 3MeOH$ (**3**·3MeOH). Complex **1** is a simple dimeric species whereas the structures of **2** and **3** are based on the decametallate $\{M_{10}O_{28}\}^{26-}$ ion. Variable-temperature direct-current (dc) magnetic susceptibility data were collected for complexes **1** and **2** in the 1.8–300 K temperature range in fields up to 5.0 T. Complex **1** has a ground state of S = 0 with the best-fit parameters $J = -12.30 \pm 0.04$ cm^{-1} and $g = 1.990 \pm 0.003$. Electronic structure calculations based on density functional theory (DFT) on **1** and **2** have been carried out and good agreement with the experimental data was found for **1**. For **2**, the theoretical results have been used as starting point to fit the J values to the experimental data, revealing the presence of competing antiferromagnetic ($J_{4,7} = -39.0$ cm^{-1}; $J_{3,7} = J_{4,6} = +1.1$ cm^{-1}, $J_{4,5} = J_{3,4} = -20.0$ cm^{-1}, $J_{3,6} = -16.0$ cm^{-1} and $J_{1,3} = J_{1,6} = J_{1,4} = J_{1,7} = -4.8$ cm^{-1}) exchange interactions between the Cr^{III} centres that suggests a singlet ground state with very close S = 1, 2, 3 and 4 excited states. Magneto-structural correlations developed on a model complex based on **1** show a strong dependence of J with Cr–O–Cr angle. A similar magneto-structural correlation is found for the J values obtained by theoretical calculations on **2**.

Introduction

Polymetallic clusters of chromium remain relatively rare, and in terms of nuclearity, relatively small. Whereas clusters of Mn, Fe, Ni, Co and Cu have, in some cases, contained more than eighty metal centres, the largest known Cr^{III} clusters contain only twelve metal ions.[1–20] The kinetically inert nature of the Cr^{III} ion usually requires reactions to be carried out at high temperatures, and the most successful synthetic routes have involved either the direct heating of the basic Cr carboxylates $[Cr_3O(O_2CR)_6(H_2O)_3]^+$ or the heating of the Cr^{III} salt in the presence of a carboxylic acid. For example, the use of a combination of CrF_3 and pivalic acid leads to a family of clusters based on wheels,[1] as does the solvothermal heating of $[Cr_3O(O_2CR)_6(H_2O)_3]^+$ in alcohol.[2] An interesting aspect of this chemistry is that homometallic Cr clusters all contain bridging carboxylates, the majority have topologies that are based on either cubes or wheels, and most are characterised by S = 0 spin ground states. The exceptions to this are a Cr_{12} centred-pentacapped trigonal prism with S = 6,[3] a ferromagnetic Cr_{10} wheel,[2] and a tetrametallic cluster with S = 6.[4]

Theoretical calculations based on density functional theory of magnetic exchange coupling constants (J) in binuclear and polynuclear transition-metal complexes have gained much attention recently because these methods have proven to give good numerical estimates of J values as well as providing insight into the electronic structure of the molecule of interest.[11,21–40] For polynuclear transition-metal complexes, the best way to experimentally obtain a good set of J values (or other spin Hamiltonian parameters such as zero-field splitting) is Inelastic Neutron Scattering (INS) or Frequency Domain Magnetic Resonance Spec-

[a] Department of Chemistry, The University of Manchester, Oxford Road, Manchester, M13 9PL, UK
[b] Departament de Química Inorgànica, Facultat de Química, Universitat de Barcelona, Diagonal 647, 08028 Barcelona, Spain
Fax: +34-93-4907725
E-mail: joan.cano@qi.ub.es
[c] Centre de Recerca en Química Teòrica, Universitat de Barcelona, 08028 Barcelona, Spain
[d] Institució Catalana de Recerca i Estudis Avançats (ICREA), Spain
[e] School of Chemistry, The University of Edinburgh, West Mains Road, Edinburgh, EH9 3JJ, UK
E-mail: ebrechin@staffmail.ed.ac.uk
Supporting information for this article is available on the WWW under http://www.eurjic.org or from the author.

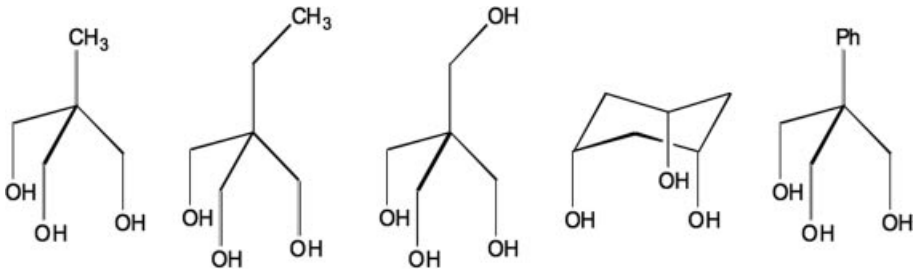

Scheme 1.

troscopy (FDMRS).[5–7] INS allows the direct spectroscopic determination (in zero-applied field) of such parameters, but unfortunately these measurements are somewhat uncommon because of restrictive sample requirements.[5] These constants can also be evaluated from magnetic susceptibility (fitting of χ_M or $\chi_M T$ vs. T curves), heat capacity or EPR measurements, but the obtained values are only correct if certain requirements are fulfilled, namely: (i) as well as in the INS experiments, the choice of an accurate spin Hamiltonian that properly describes the magnetic properties of the system; (ii) the presence of critical points in the experimental curves that allow for a better assessment of the variable parameters in the fitting; and (iii) avoidance of over-parameterisation, i.e. using too many parameters (J constants) in the spin Hamiltonian. In this latter case, obtaining a set of J values from theoretical calculations as a starting point for the fitting procedure is a very useful alternative.

We have been using the tripodal ligand 1,1,1-tris(hydroxymethyl)ethane (H_3thme, Scheme 1) and its analogues in the synthesis of Mn, Fe, Ni and Co clusters[8] and herein report our first attempts to make polymetallic Cr^{III} clusters including a novel dinuclear cluster and a related octametallic Cr^{III} cluster whose structure is based on the decametallate $\{M_{10}O_{28}\}^{26-}$ ion. Both complexes are formed from similar reaction schemes, but the dimeric cluster is isolated under reflux and the octametallic species isolated under solvothermal conditions. In order to elucidate the magnetic properties of these compounds, we have also studied their electronic structure. The relevant exchange coupling constants have been calculated and several magneto-structural correlations have been found and interpreted according to the Cr–O–Cr angle for different families displaying several bridging ligands (oxo, alkoxo).

Results and Discussion

Synthesis

When $CrCl_2$, H_3tmp and NaOMe are stirred in MeOH at room temperature no isolable products are obtained, even if the solvent is evaporated and the resultant solid extracted into a variety of solvents. When the reaction is repeated, but under reflux, the dimeric species **1** is obtained when the original MeOH solution is stripped off and the resultant solid redissolved in MeCN. No isolable product is obtained from the initial MeOH solution or from any other solvents, or when the reaction is repeated with the tripodal ligands H_3thme or H_4peol. Superheating a methanolic solution containing equivalent amounts of $CrCl_2$, H_3thme or H_4peol and NaOMe in a sealed high-pressure vessel at 100 °C for 12 h followed by slow cooling to room temperature generates crystals of compounds **2** and **3**, respectively, directly from the reaction mixture in high yield. It is likely that the Cr^{II} ions are oxidised almost immediately upon dissolution, but the analogous reactions – under both refluxing and solvothermal conditions – using Cr^{III} halides failed to yield any isolable products.

Structure Description

Complex **1** (Figure 1) crystallises in the monoclinic space group $P2_1/c$. Selected bond lengths and angles are given in Table 1. The structure consists of two Cr^{III} ions related by an inversion centre, bridged by two singly deprotonated H_2tmp^- ligands. The deprotonated arms (O1 and O1A) act as μ-bridges with the protonated arms (O2, O3A and symmetry equivalents), each bonding in a terminal fashion. These are H-bonded to the MeOH solvent molecules [e.g. O4···O2, 2.552(3) Å] and their bonds to Cr are slightly longer [1.983(2)–2.017(2) Å] than the bridging Cr–O distances [1.954(2)–1.964(2) Å]. Two terminal chloride ions (Cl1, Cl2 and symmetry equivalents) complete the coordination spheres of the Cr^{III} ions, and these H-bond to the

Figure 1. Perspective view of the dinuclear complex $[Cr_2(H_2tmp)_2Cl_4]$ (**1**).

Table 1. Selected bond lengths, intermetal distances and angles for **1**.

Cr1–O1	1.954(2)	Cr1–Cl1	2.338(2)
Cr1–O1A	1.964(2)	Cr1–Cl2	2.309(2)
Cr1–O2	1.983(2)	Cr1···Cr1A	3.022(2)
Cr1–O1–Cr1A	100.9(2)	O1A–Cr1–Cl1	173.1(1)
O1–Cr1–O1A	79.1(2)	O2–Cr1–Cl1	90.0(2)
O1–Cr1–O2	90.6(2)	O3–Cr1–Cl1	91.4(2)
O1A–Cr1–O2	87.8(2)	O1–Cr1–Cl2	171.8(2)
O1–Cr1–O3	86.9(2)	O1A–Cr1–Cl2	93.5(2)
O1A–Cr1–O3	90.5(2)	O2–Cr1–Cl2	92.6(2)
O2–Cr1–O3	177.3(2)	O3–Cr1–Cl2	89.7(2)
O1–Cr1–Cl1	94.4(2)	Cl1–Cr1–Cl2	93.2(1)

oxygen arms of the tripodal ligands on neighbouring molecules (Cl···O, 3.06–3.18 Å). The Cr^{III} ions are in distorted octahedral geometries with *cis* angles in the range 79.1(1)–94.43(7)° and *trans* angles of 171.77(7)–177.25(9)°. In the crystal the Cr_2 units pack in 2D sheets as mediated by the Cl···O and O(tripod)···O(MeOH) H-bonds, with these "metallic" sheets separated from each other by the organic tails of the tripodal ligands and the chloride ions. Here, the closest intermolecular interactions are of the order 3.5–4.0 Å. Complex **1** is structurally related to the vanadium dimers of general formula $[V_2O_2(H_2tripod)_2Cl_2]$, in which one of the chloride ions on each metal has been replaced by an oxygen.[9]

Complex **2**, $[Cr_8O_2(thme)_2(Hthme)_4Cl_6]$ crystallises in the triclinic space group $P\bar{1}$, whereas complex **3**, $[Cr_8O_2(Hpeol)_2(H_2peol)_4Cl_6]$ crystallises in the monoclinic space group $C2/c$. Both structures are essentially the same, and thus we will confine our discussion to complex **2** (Table 2 and Table 3). Differences in the packing arrangements between **2** and **3** are discussed afterwards (Figure S1). The core of **2** (Figure 2) consists of two $[Cr_5O]^{13+}$ square-based pyramids, related by an inversion centre, which share one edge forming a central $[Cr_8O_2]^{20+}$ unit. The core can be regarded as part of the decametallate $\{M_{10}O_{28}\}^{26-}$ ion of two edge-sharing octahedra, but with two of the apical metal centres missing and with the bridging and terminal oxo groups replaced by a combination of oxygen atoms from tripodal ligands and chloride ions. The tripodal ligands are of two types: the two fully deprotonated $thme^{3-}$ ligands, each bound to the open triangular face of the square-based pyramid with each oxygen (O5, O6, O10A) arm bridging in a μ_2-fashion between either the apical Cr^{III} ion (e.g. Cr3A) and basal ion (e.g. Cr2) or between two basal Cr^{III} ions (e.g. Cr4A, Cr2). The remaining four tripodal ligands are doubly deprotonated, $Hthme^{2-}$, and occupy four of the "faces" surrounding the vacant apical Cr sites: one deprotonated arm bonds in a μ_2-fashion between apical and basal Cr^{III} ions (e.g. O9) – thus linking the two square-based pyramids together; the second deprotonated arm bridges between two basal sites (e.g. O8), with the third protonated arm (e.g. O7) binding in a terminal fashion to a basal Cr^{III} site. There are six chloride ions in the structure which each bond terminally to Cr^{III} ions on the open triangular faces of the square-based pyramids. The two O^{2-} ions are five-coordinate and square-based pyramidal, each bound to four basal and one apical Cr^{III} ion, with *cis* angles in the range 89.2–95.3° and *trans* angles 170.8–172.0° (Table 2). The result is an $\{M_8L_{26}\}$ unit, equivalent to the $\{M_{10}O_{28}\}^{26-}$ decametallate ion minus the two {ML} apices. The terminal Cr–O bonds of the $Hthme^{2-}$ ligand are significantly longer (2.020–2.064 Å) than the μ-bridging oxygen

Table 2. Selected bond lengths and angles for **2**.

Cr1–O1	2.084(2)	Cr2–O5	1.963(3)	Cr3–O9	1.979(3)
Cr1–O1A	2.087(2)	Cr2–O6	1.962(3)	Cr3–O10	1.971(3)
Cr1–O2	1.958(3)	Cr2–O7	2.064(3)	Cr4–O1	2.108(2)
Cr1–O3	1.928(3)	Cr2–O8	1.978(3)	Cr4–O3	1.961(3)
Cr1–O8	1.933(3)	Cr3–O1	2.060(3)	Cr4–O4	2.020(3)
Cr1–O9	1.977(3)	Cr3–O2	1.978(3)	Cr4–O6	1.950(3)
Cr2–O1	2.083(2)	Cr3–O5	1.984(3)	Cr4–O10	1.954(3)
Cr2–Cl1	2.273(1)	Cr3–Cl2	2.292(1)	Cr4–Cl3	2.282(1)
Cr1–O1–Cr1A	89.3(1)	Cr1–O1–Cr2	170.9(1)	Cr1–O1–Cr3	95.2 (1)
Cr1–O1–Cr4	89.1(1)	Cr2–O1–Cr3	93.9 (1)	Cr2–O1–Cr4	90.4(1)
Cr3–O1–Cr4	93.6(1)	Cr1–O1A–Cr2	89.9(1)	Cr1–O1A–Cr3	94.3(1)
Cr1–O1A–Cr4	172.1(1)	Cr3–O1A–Cr4	101.5(1)	Cr1–O2–Cr3	101.1(1)
Cr2–O5–Cr3	100.2(1)	Cr2–O6–Cr4	99.0(1)	Cr1–O8–Cr2	97.7(1)
Cr1–O9–Cr3	101.36(1)	O1–Cr1–O8	172.7(1)	O1A–Cr1–O3	173.5(1)
O2–Cr1–O9	172.9(1)	O1–Cr1–O3	87.0 (1)	O1A–Cr1–O8	86.7(1)
O1A–Cr1–O9	93.2(1)	O3–Cr1–O8	96.3(1)	O3–Cr1–O9	92.54(1)
O5–Cr2–O7	170.8(1)	O6–Cr2–O8	170.4 (1)	O1A–Cr2–Cl1	179.22(1)
O1A–Cr2–O6	85.4(1)	O1A–Cr2–O8	85.6(1)	O5–Cr2–O8	92.1(1)
O6–Cr2–O7	89.7(1)	O6–Cr2–Cl1	93.9(1)	O7–Cr2–Cl1	92.2(2)
O2A–Cr3–O10	165.1(1)	O5A–Cr3–O9	165.0(1)	O1–Cr3–Cl2	179.5(1)
O1–Cr3–O2A	82.4(1)	O2A–Cr3–O9	85.5(1)	O5A–Cr3–O10	88.9(1)
O9–Cr3–O10	90.0(1)	O9–Cr3–Cl2	98.3(1)	O10–Cr3–Cl2	96.8(1)
O3–Cr4–O6A	169.3(1)	O4–Cr4–O10	172.7(1)	O1–Cr4–Cl3	177.1(1)
O1–Cr4–O3	85.5(1)	O1–Cr4–O6A	85.0(1)	O1–Cr4–O10	82.0(1)
O3–Cr4–O10	93.2(1)	O6A–Cr4–Cl3	95.6(1)	O10–Cr4–Cl3	95.1(1)

Table 3. Selected bond lengths, intermetal distances and angles for **3**.

Cr1–O1	2.088(2)	Cr2–O2	1.988(2)	Cr3–O8A	1.955 (2)
Cr1–O1A	2.086(2)	Cr2–O4	2.039(2)	Cr3–O10	1.964(2)
Cr1–O2	1.937(2)	Cr2–O8	1.951(2)	Cr4–O1A	2.040(2)
Cr1–O3	1.968(2)	Cr2–O9	1.960(2)	Cr4–O3	1.978(2)
Cr1–O5	1.924(2)	Cr3–O1A	2.116(2)	Cr4–O6A	1.978 (2)
Cr1–O6	1.959(2)	Cr3–O5	1.972(2)	Cr4–O9A	1.983(2)
Cr2–O1	2.080(2)	Cr3–O7	2.008(2)	Cr4–O10	1.971(2)
Cr2–Cl1	2.286(1)	Cr3–Cl2	2.268(1)	Cr4–Cl3	2.297(1)
Cr1···Cr1A	2.931(1)	Cr1···Cr2	2.937(1)	Cr1···Cr3	2.949(1)
Cr1···Cr4	3.033(1)	Cr1···Cr4A	3.037(1)	Cr2···Cr3A	2.988(1)
Cr2···Cr4	3.026(1)	Cr3···Cr4	3.025(1)	O11···O13	2.656(1)
Cr1–O1–Cr1A	89.2(1)	Cr3A–O1–Cr4A	93.4(1)	Cr1A–O1–Cr2	170.9(1)
Cr1–O1–Cr2	89.6(1)	Cr1–O2–Cr2	96.9 (1)	Cr1–O1–Cr3A	171.9(1)
Cr1A–O1–Cr3A	89.1(1)	Cr2–O1–Cr3A	90.8 (1)	Cr1–O1–Cr4	94.7(1)
Cr2–O1–Cr4A	94.6(1)	Cr1A–O1–Cr4A	94.6(1)	Cr1–O3–Cr4	100.4(1)
Cr1–O5–Cr3	98.4(1)	Cr1–O6–Cr4A	100.9(1)	Cr2–O8–Cr3A	99.8(1)
Cr2–O9–Cr4A	100.24(1)	O1–Cr1–O5	173.7(1)	O1A–Cr1–O2	173.2(1)
O3–Cr1–O6	173.4(1)	O1–Cr1–O1A	90.8(1)	O1–Cr1–O2	87.2(1)
O1–Cr1–O3	93.3(1)	O1A–Cr1–O3	82.0(1)	O1A–Cr1–O5	87.2(1)
O1A–Cr1–O6	93.5(1)	O2–Cr1–O5	95.4(1)	O3–Cr1–O6	92. 4(1)
O2–Cr2–O8	170.9(1)	O4–Cr2–O9	171.9(1)	O3–Cr2–Cl1	178.9(1)
O1–Cr2–O2	86.1(1)	O1–Cr2–O4	89.5(1)	O1–Cr2–O8	85.2(1)
O2–Cr2–O9	91.6(1)	O4–Cr2–Cl1	90.9(1)	O3–Cr2–Cl1	93.8(1)
O5–Cr3–O8A	168.4(1)	O7–Cr3–O10	171.2(1)	O1A–Cr3–Cl2	178.2(1)
O1A–Cr3–O5	85.2(1)	O1A–Cr3–O8A	84.1(1)	O5–Cr3–O7	87.8(1)
O5–Cr3–O10	92.9(1)	O7–Cr3–Cl2	92.6(10)	O8A–Cr3–Cl2	96.6(1)
O3–Cr4–O9A	165.7(1)	O6A–Cr4–O10	166.5(1)	O1A–Cr4–Cl3	178.3(1)
O1A–Cr4–O6A	82.6(1)	O3–Cr4–O6A	86.2(1)	O3–Cr4–O10	91.0(1)
O9A–Cr4–O10	96.7(1)	O3–Cr4–Cl3	95.5(1)	O9A–Cr4–Cl3	98.7(1)

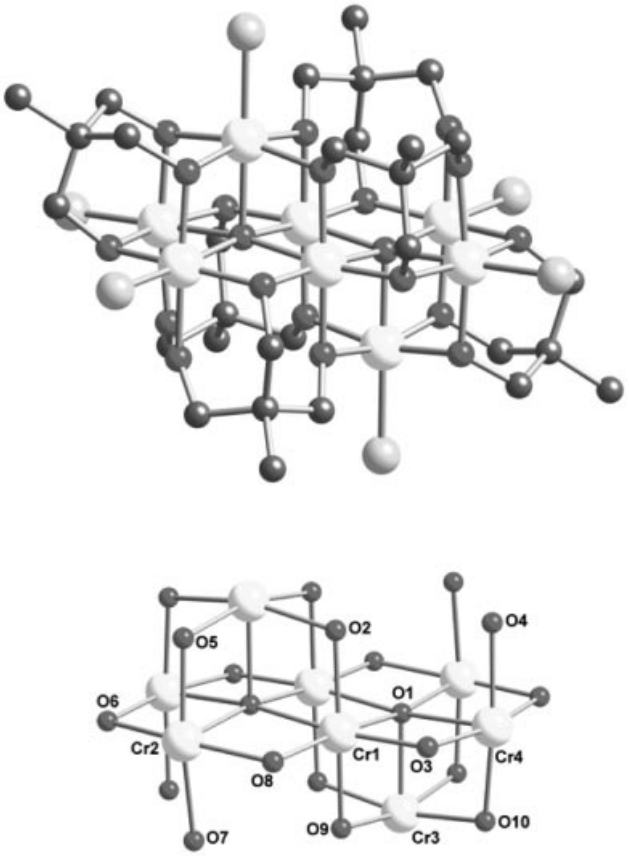

Figure 2. Perspective view of the octanuclear complex $[Cr_8O_2(thme)_2(Hthme)_4Cl_6]$ (**2**) (top) and its metal–oxygen core (bottom).

bond lengths (1.949–1.984 Å), with O4 and O7A hydrogen bonded both to each other and a MeOH solvate molecule (e.g. O4···O7A, 2.737 Å; O4···O11, 2.662 Å) (Table 2). All the Cr^{III} ions are in distorted octahedral geometries with their oxidation states confirmed by a combination of BVS calculations, bond lengths and overall charge balance considerations.

In the crystal the molecules pack in columns with one Cr_8 unit sitting directly above and below its nearest neighbours. Here, the closest intermolecular interactions are between the terminal chloride ions and the tripodal ligands (≈ 3.5–3.7 Å). Intermolecular interactions between the columns are mediated through a combination of Cl···C (tripod) H-bonds (in the region of ≈ 3.5–3.7 Å), and the Cl···O (MeOH) H-bonds. For complex **3**, the pendant alcohol group of the pentaerythritol ligand is found to greatly influence the packing within the crystal lattice. These additional OH groups form hydrogen bonds to molecules in adjacent planes (e.g. O11···O13, O11A···O13A) at a distance of ca. 2.65 Å and result in these planes packing in a perpendicular fashion. The terminal chloride ions are also involved in two intermolecular H-bonding interactions; one OH···Cl interaction with an uncoordinated H_2peol^- ligand arm (e.g. O12···Cl3, 3.25 Å), and the other with a MeOH solvent molecule (O17···Cl2, 3.21 Å).

The edge-sharing $[M_8(\mu_5\text{-}O_2)]^{n+}$ core adopted by **2** and **3** is somewhat unusual. Other examples of this octanuclear fragment are restricted to the Ba clusters $[Ba_8O_2]^{12+}$, $[Sr_6Ba_2O_2]^{12+}$ and $[Ba_8Eu_2O_2]^{12+}$ where the principal bridging ligand is also an alkoxo group.[10,11] Similar cores can, however, be found in the decanuclear transition-metal

clusters $[Fe_{10}O_2Cl_8(tmp)_6]$, $[(VO)_2Fe_8O_2Cl_6(tmp)_6]$ and $(NEt_4)_2[Mn_{10}O_2Cl_8(thme)_6]$.[9,12,13]

Magnetic Measurements

Solid-state dc magnetisation measurements were performed on **1** and **2** in the temperature range 1.8–300 K in a field of 5.0 kG and the Irreducible Tensor Operator (ITO) formalism was employed to fit the experimental data by means of the programme VPMAG.[14] For complex **1**, the room temperature $\chi_M T$ value of approximately 3.75 $cm^3 \cdot K \cdot mol^{-1}$ is that expected for two non-interacting Cr^{III} centres (Figure 3). As the temperature is lowered, the value of $\chi_M T$ drops very gradually until approximately 100 K where it begins to fall more dramatically, reaching a value close to 0 $cm^3 \cdot K \cdot mol^{-1}$ at 1.8 K. At 27 K a maximum in χ_M is reached (χ_M = 0.0512 $cm^3 \cdot K \cdot mol^{-1}$). This behaviour is indicative of relatively weak antiferromagnetic exchange coupling between the Cr^{III} ions with an $S = 0$ spin ground state. Using the spin Hamiltonian $\hat{H} = -J\hat{S}_1 \cdot \hat{S}_2$, the best fit (Figure 3 solid line) was obtained for the following parameters: $J = -12.30 \pm 0.04$ cm^{-1} and $g = 1.990 \pm 0.003$, resulting in an S = 0 spin ground state. The agreement factor of the fit, defined as

$F = \{\Sigma[\chi_i^{exp.} - \chi_i^{calcd.}]^2\}/\{\Sigma[\chi_i^{calcd.}]^2\}$, is good ($F = 1.1 \cdot 10^{-5}$).

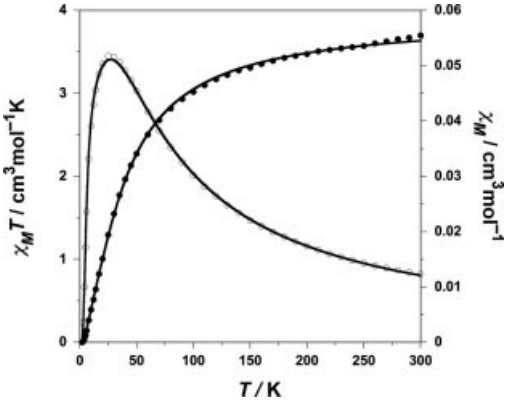

Figure 3. Plot of χ_M and $\chi_M T$ vs. T for complex **1**. The solid lines are fits to the experimental data. See text for details.

For complex **2**, the $\chi_M T$ value of approximately 10.8 $cm^3 \cdot K \cdot mol^{-1}$ at 300 K is smaller than that expected for eight noninteracting $S = 3/2$ metal centres (15 $cm^3 \cdot K \cdot mol^{-1}$, with $g = 2.0$). Below 300 K, the value of $\chi_M T$ drops gradually with temperature reaching a pseudo-plateau with a value of approximately 3.2 $cm^3 \cdot K \cdot mol^{-1}$ at 10 K (Figure 4). This behaviour is indicative of dominant antiferromagnetic exchange between the Cr^{III} ions, resulting in a relatively small spin ground state ($S = 2$). Below 10 K the $\chi_M T$ value falls again to approximately 2 $cm^3 \cdot K \cdot mol^{-1}$ at 1.8 K. The decrease of $\chi_M T$ in this last region is probably due to intermolecular interactions, the magnetic anisotropy of the ground spin state, or (less probably) the presence of more stable states displaying lower spin angular momenta.

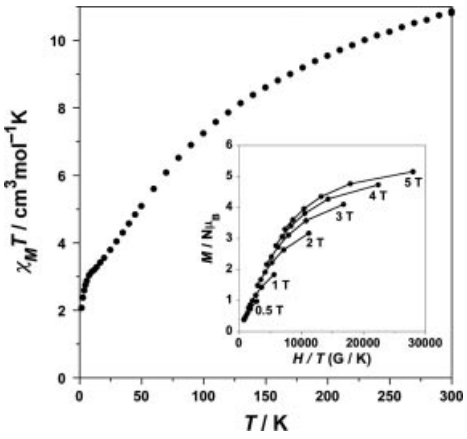

Figure 4. Plot of $\chi_M T$ vs. T for complex **2** and (inset) magnetisation (M) vs. field (H) data taken in the ranges 1.8–6.2 K and 0.5–5.0 T.

Magnetisation measurements in the 1.8–6.2 K temperature range were performed under constant magnetic fields of 0.5–5.0 T (Figure 4, inset). The isofield lines are not superimposable and the values of reduced magnetisation ($M/N\mu_B$) become higher than expected for the postulated spin ground state ($M/N\mu_B \approx 4$ for $S = 2$). This is probably caused by population of low-lying excited states with higher spin numbers which become more stable with increasing fields. For this reason a fit of the magnetisation data to a Brillouin equation was not attempted, because a well-isolated spin ground state is required for such a model to apply. The possibility of slow relaxation of the magnetisation was investigated by collection of ac susceptibility data taken in a range of frequencies. However, no out-of-phase (χ_M'') signal was observed over the whole temperature range (1.8–6.2 K) indicating that **2** is not a single-molecule magnet.

Unfortunately, there are few examples of Cr^{III} compounds in the literature that actually possess similar bridging ligands to the ones found in **2** and **3**, and even these contain other bridging co-ligands (e.g. carboxylates etc.).[15–23] Moreover, there exists little magnetic characterisation of these species and/or their magnetic properties have not been quantitatively analysed because the complexity of the system.[24–30] Thus, it is very difficult to compare and contrast any results with other Cr^{III} complexes. In addition, in such complicated multiple J systems it is usually possible to find several sets of J values that can reproduce the experimental magnetic behaviour equally well. We therefore decided to carry out calculations based on DFT in order to either have good estimated J values to use them as a starting point in a fit.

Theoretical Study of the Magnetic Exchange Coupling

Complex 1

An exchange coupling constant, $J = -7.5$ cm^{-1}, has been obtained from DF calculations on complex **1** using the broken symmetry approach. Although the theoretical study correctly reproduces the nature of the magnetic interaction, the magnitude of the J constant is slightly lower than the

experimental value (–12.3 cm^{-1}). Despite the fact that only a few compounds display the $[Cr_2(OX)_2]^{4+}$ core (X = H, Me or Et), there does exist a magneto-structural correlation for this unit based on experimental structural parameters which relates the magnetic exchange constant to the Cr–O–Cr angle (α), the Cr–O distance (d_{CrO}), and the dihedral angle formed between the OR group and Cr_2O_2 plane (θ).[31] Here, we have revisited this correlation bringing up to date the experimental data (Table 4), as well as performing a theoretical analysis by electronic structure calculations. The Cr–O distance remains essentially unchanged along the series of compounds, so we have focused our efforts in the study of the influence of the α and θ angles. We have used the model complex $[Cr_2(OMe)_2(H_2O)_4Cl_4]$ (**1A**) built from the experimental structural parameters of **1** (Figure S2). In this magneto-structural correlation only the α angles have been modified with the remaining parameters constant. It is important to stress that the molecular geometry of the most stable compound corresponds to an α angle equal to 100.85° – similar to that experimentally found (100.93°, Figure 5). This α value is the same in the singlet (ground state) and triplet state. The thermal energy at room temperature allows the α angle to achieve any value between 98.8 and 102.8° and so, in agreement with the experimental data (Table 4), we can conclude that the experimental α angles in the $[Cr_2(OR)_2]^{4+}$ complexes will take similar values.

At α = 101.3° (α_{min}), near the more stable molecular geometry, the antiferromagnetic exchange coupling reaches a minimum value (J = –5.2 cm^{-1}). At lower α angles the exchange coupling becomes strongly antiferromagnetic because the inter-metal distance is short enough to allow direct interaction between the paramagnetic centres ($\alpha < 95°$). However, as has been observed in bis-alkoxo dinuclear copper(II) complexes,[32,33] there is an experimental and theoretical correlation between the α and θ (dihedral) angles (Figure S3). However, no qualitative changes occur in the magneto-structural correlation between the J constant and the α angle (Figure 5). Most complexes display an α value of around 100–101°, but in some cases where bulky alkoxo bridging ligands are used, the α angle can take larger values.

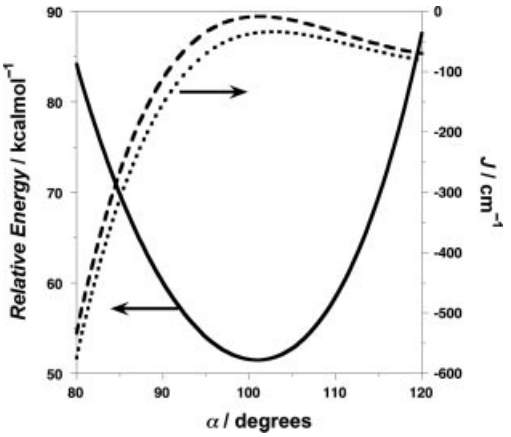

Figure 5. Relative energy (in kcal/mol, solid line) of the singlet ground state and magnetic exchange coupling as a function of the bridging angle Cr–O–Cr (α) angle. The dotted and dashed lines correspond to the J values obtained on model **1A** when the θ angle is or is not optimised, respectively.

In these cases the alkoxo group is almost coplanar with the $[Cr_2(OR)_2]^{4+}$ unit and the antiferromagnetic coupling becomes stronger (Table 4), as predicted by theoretical calculations.[22,34–41] We have analysed this magneto-structural correlation in order to find the electronic factors that govern it (Figure S4). In agreement with previous work, we have concluded that the contribution from the d_{xy} magnetic orbitals is responsible for the correlation between the J constant and the α angle.[31] A more detailed analysis can be found in the Supporting Information.

The thme ligand provides two possible exchange pathways to mediate the magnetic exchange coupling between the Cr^{III} centres: (a) by one alkoxo oxygen only; and (b) by the more extended O–C–C–C–O network (see Figure 1). In previous work, we demonstrated that the more extended pathway is an inefficient route for magnetic communication between Fe^{III} ions where t_{2g} and e_g magnetic orbitals are present.[42] In this case, calculations on the full experimental molecule and on the simpler model lead to the same conclusion. The calculations on the model, where only the shortest pathway is present, give a theoretical J value (–5.2 cm^{-1})

Table 4. Experimental structural data and exchange coupling constants[a] for $[Cr_2(OR)_2]^{4+}$ compounds.

Compound	d_{CrO}	α	θ	J[b]	Refcode[c]	Ref.
$[Cr(L_1)(Cl)]_2(ClO4)_2$·DMF	1.963	99.27	149.77	–	FEBXIT	[36]
$[Cr(L_2)(OMe)(H_2O)]_2(ClO4)_2$	1.958	100.79	154.07	–	DESRIC	[37]
$[Cr(H_2tmp)Cl_2]_2$·2MeOH	1.959	100.93	142.93	–12.3 (–7.5)	–	this work
$[Cr(acac)_2(OMe)]_2$	1.962	101.03	150.19	–9.8	BIKVAS	[22]
$[Cr(3\text{-}Cl\text{-}acac)_2(OMe)]_2$	1.959	101.09	155.58	–9.8	MXCACR10	[34]
$[Cr(3\text{-}Br\text{-}acac)_2(OMe)]_2$	1.956	101.44	154.48	–8.5	MXBACR10	[34]
$[Cr(tmjd)_2Cr(OMe)]_2$	1.954	101.74	148.77	–8.9	CUVVAQ	[38]
$[Cr(3\text{-}Br\text{-}acac)_2(OEt)]_2$	1.958	101.75	161.58	–17.9	EXBACR10	[34]
$[Cr(DpyF)(OMe)(Cl)]_2$	1.977	101.88	159.69	–12.5	WOXFIY	[39]
$[Cr(L^S)(OMe)(MeOH)]_2$·MeOH	1.981	103.10	175.41	–16.6	VACROH	[40]
$[Cr(L^{Se})(OMe)(MeOH)]_2$	1.968	103.58	177.32	–18.0	VACREX	[40]
$[Cr(L_3)(MeOH)]_2$·MeOH	1.984	104.17	167.07	–	QOZRIG	[41]

[a] All angles in °; distance in Å and constants in cm^{-1}. [b] Because various magnetic models have been used in the literature, J refers to the energy of the triplet states as calculated from the observed susceptibility data. Theoretical value obtained from electronic structure calculations is in parentheses. [c] Codes for locating structural data in the Cambridge Structural Database.[58]

similar to that obtained for the full molecule (–7.5 cm^{-1}). Moreover, the experimental J value of **1** (–12.3 cm^{-1}) agrees well with those observed in previous complexes presenting similar α angles via the shortest M–O–M pathway only (–9.8 cm^{-1}). Therefore, the longest M–O–C–C–C–O–M pathway should not be relevant in these complexes as it leads to weak contributions. The contribution of e_g magnetic orbitals – not present in the Cr^{III} ion – are mainly responsible for the magnetic exchange coupling in Fe^{III} complexes and it is strongly weakened when the exchange pathway is lengthened.

Complex 2

As was shown in the structural section, the metal ions in complexes **2** and **3** are connected in three different ways: (a) by two μ_5-oxo bridging ligands (J_1); (b) by one μ_5-oxo ion (J_2); and (c) by one μ_5-oxo ion and one μ-alkoxo (J_3). However, this simple model infers a higher molecular symmetry than that experimentally found (Figure 6). The lower molecular symmetry is related to the different Cr–O bond lengths and Cr–O–Cr angles, and in reality we can take into account ten possible exchange coupling constants and, thus, the spin Hamiltonian (Equation (1):

$$\hat{H} = -J_{4,7}\hat{S}_4 \cdot \hat{S}_7 - J_{3,7}(\hat{S}_3 \cdot \hat{S}_7 + \hat{S}_4 \cdot \hat{S}_8) - J_{4,6}(\hat{S}_4 \cdot \hat{S}_6 + \hat{S}_5 \cdot \hat{S}_7) - J_{4,5}(\hat{S}_4 \cdot \hat{S}_5 + \hat{S}_6 \cdot \hat{S}_7) - J_{3,4}(\hat{S}_3 \cdot \hat{S}_4 + \hat{S}_7 \cdot \hat{S}_8) - J_{3,6}(\hat{S}_3 \cdot \hat{S}_6 + \hat{S}_5 \cdot \hat{S}_8) - J_{1,3}(\hat{S}_1 \cdot \hat{S}_3 + \hat{S}_2 \cdot \hat{S}_8) - J_{1,6}(\hat{S}_1 \cdot \hat{S}_6 + \hat{S}_2 \cdot \hat{S}_5) - J_{1,4}(\hat{S}_1 \cdot \hat{S}_4 + \hat{S}_2 \cdot \hat{S}_7) - J_{1,7}(\hat{S}_1 \cdot \hat{S}_7 + \hat{S}_2 \cdot \hat{S}_4) \quad (1)$$

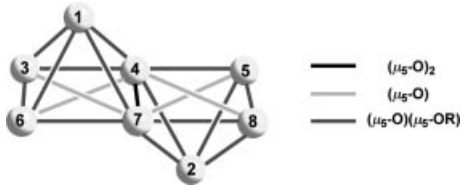

Figure 6. Scheme of the interactions employed in the study of the magnetic properties of **2** and **3**.

where the subindex in the J constants refers to the paramagnetic centres involved in the exchange coupling. We have performed a least-squares fitting to the fourteen-equation system obtained from the differences in the energy between the fifteen spin distributions (SD_i) shown in Table S1. The results are shown in the Table 5. In Figure 7 is displayed a spin density map of the most stable configuration, SD_3. A more detailed description of this study is able in the Supporting Information.

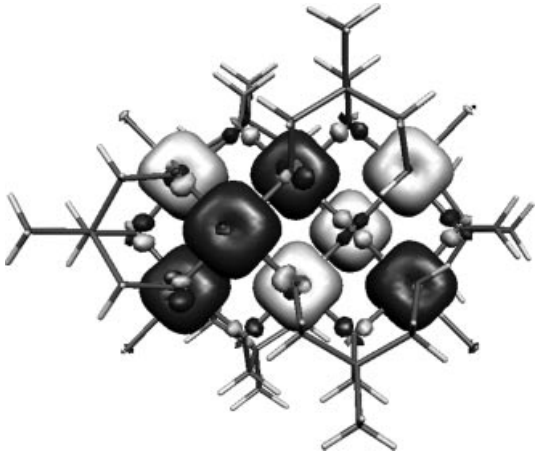

Figure 7. Spin density map calculated at the B3LYP level for the spin ground state of **2** (light and dark contours indicate positive and negative spin populations, respectively). The isodensity surface corresponds to a value of 0.005 $e^-/bohr^3$.

Although the $[Cr_2O_2]$ unit has a relatively low symmetry, a good magneto-structural correlation is found between the exchange coupling constants and the Cr–O–Cr angle in the cases where one oxo and one alkoxo groups act as bridges between metal ions (interaction 4–5, 3–4, 3–6, 1–3. 1–6, 1–4, 1–7; see Table 5). A change of the nature of the magnetic interaction is observed at α ca. 98°, where the ferro- and antiferromagnetic contributions are counter-balanced and a zero value for the J constant is expected (Figure 8). This correlation is also found with the metal–metal distance because the Cr–O distances are almost constant within this small family. Only one system is not in accord with this correlation, displaying a weaker antiferromagnetic interaction than that expected, probably due to the longer Cr–O bond length (2.026 Å, Table 5) weakening the metal–ligand overlap and thus the magnetic exchange.

Table 5. Description of the bridging ligands, average Cr···Cr distances, Cr–O bond lengths, Cr–O–Cr bond angles and calculated exchange coupling constants $J_{i,j}$ (in cm^{-1}).

i,j	Bridging ligands	d(Cr···Cr)[a]	d(Cr–O)[a]	Cr–O–Cr (α)[a]	$J_{i,j}$
4,7	$(\mu_5\text{-}O^{2-})_2$	2.930 (2.930)	2.085 (2.087)	89.3 (89.2)	–52.7
3,7	$(\mu_5\text{-}O^{2-})$	4.154 (4.152)	2.084 (2.083)	170.9 (170.9)	–3.8
4,6	$(\mu_5\text{-}O^{2-})$	4.165 (4.194)	2.097 (2.102)	172.1 (171.9)	–2.8
4,5	$(\mu_5\text{-}O^{2-})(\mu\text{-OR})$	2.942 (2.949)	2.021 (2.025)	93.7 (93.8)	–26.2
3,4	$(\mu_5\text{-}O^{2-})(\mu\text{-OR})$	2.946 (2.937)	2.020 (2.023)	93.8 (93.3)	–25.7
3,6	$(\mu_5\text{-}O^{2-})(\mu\text{-OR})$	2.974 (2.987)	2.026 (2.026)	94.7 (95.3)	–10.6
1,3	$(\mu_5\text{-}O^{2-})(\mu\text{-OR})$	3.029 (3.026)	2.023 (2.020)	97.1 (97.4)	–4.8
1,6	$(\mu_5\text{-}O^{2-})(\mu\text{-OR})$	3.039 (3.025)	2.023 (2.023)	97.6 (96.9)	–3.9
1,4	$(\mu_5\text{-}O^{2-})(\mu\text{-OR})$	3.039 (3.033)	2.021 (2.017)	97.7 (97.8)	–1.4
1,7	$(\mu_5\text{-}O^{2-})(\mu\text{-OR})$	3.061 (3–037)	2.023 (2.018)	98.3 (97.5)	+0.8

[a] The values corresponding to **3** are displayed in parentheses. Angles and distances are given in ° and Å.

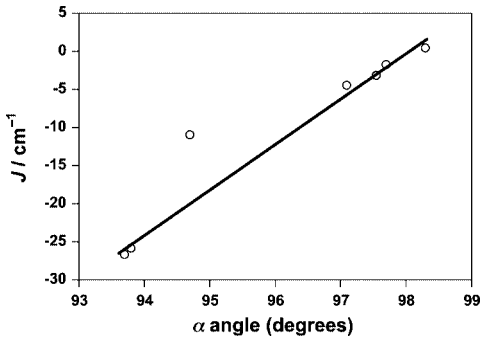

Figure 8. Dependence of the calculated exchange coupling constant (J) in **2** for the $[Cr_2O_2]^{2+}$ core with the Cr–O–Cr(α) angle.

There are two exchange interactions that mediate only through one μ_5-oxo bridge (interaction 3–7, 4–6; see Table 5) where the J constants are found to be –3.8 cm^{-1} and –2.8 cm^{-1}. These values are very similar because both $[Cr_2O_2]$ units have similar α values (170.9° and 172.1°). The magnetic coupling in this case is expected to be governed by the Cr–O distance, so the stronger of the two J constants is the one with the shortest Cr–O bond length. The stronger magnetic interactions found in **2** where two μ_5-oxo bridges are present (interaction 4–7) should thus be due to the extremely small α values (Table 5).

Unfortunately, it is difficult to find similar compounds in the literature that have been structurally and magnetically characterised. In fact, only two such dinuclear complexes and one dodecanuclear Cr^{III} complex exist.[17,29,30] For the dinuclear complexes there are no reported magnetic measurements and for the Cr_{12} cluster the measurements have not been analysed due to the complexity of the system. The crystal structures of two Cr^{III} dimers displaying a linear or quasi-linear $[Cr_2O]^{4+}$ core are known,[24,25] but, as is often the case, there are no studies of the magnetic properties, meaning we have no way to check the validity of our theoretical results.

The magnetic behaviour of **2** can be simulated by exact diagonalisation of the energy matrix built using the irreductible tensors operator approach. We have obtained the $\chi_M T$ vs. T curve for **2** from the calculated J values and find that they are in qualitatively acceptable agreement with the experimental curve (Figure 9). We have also carried out a fit using these J values as starting point and to avoid overparameterisation, we have reduced the number of variables in the way shown in Table 6. The best fit was obtained for the following parametes: $J_{4,7}$ = –39.0 cm^{-1}; $J_{3,7}$ = $J_{4,6}$ = +1.1 cm^{-1}, $J_{4,5}$ = $J_{3,4}$ = –20.0 cm^{-1}, $J_{3,6}$ = –16.0 cm^{-1}, $J_{1,3}$ = $J_{1,6}$ = $J_{1,4}$ = $J_{1,7}$ = –4.8 cm^{-1} and g = 1.919. The J values are in good agreement with the calculated ones. However, the g factor is slightly smaller than that expected for a chromium(III) ion (1.98–1.99). This fact can be explained by a partial hydration of the sample observed when it is exposed to the environment modifying the formula mass. According to the magneto-structural correlation observed in **2** (Figure 8), when one oxo and one alkoxo group act as bridges, a strong antiferromagnetic coupling is expected for small angles (89.3°) such as it occurs for $J_{4,7}$. Probably, for this α value a short metal–metal distance is found favouring the direct interaction between two metal ions, as proposed in the previous theoretical study on dinuclear models (compound **1**). It is also possible to find a set of J parameters with a g factor near to 1.98–2.00; however, this set is discarded because the obtained $J_{4,7}$ value is too large (–122.9 cm^{-1}). In fact, the $J_{4,7}$ value expected from the magneto-structural correlation shown in Figure 8 (–53.3 cm^{-1}) is lower and closer to that obtained from DF calculations. In the curves obtained with the calculated and fitted J values, as the temperature decreases the value of $\chi_M T$ is close to reaching a plateau ($\chi_M T \approx 3.2$ $cm^3 \cdot K \cdot mol^{-1}$) in agreement with the experimental curve. At lower temperatures the value of $\chi_M T$ falls to reach a value equal to zero corresponding to a singlet ground state. Thus, we can reject possible intermolecular interactions or magnetic anisotropy as a cause of the magnetic behaviour at lower temperature. Regardless, the chosen set of J values must explain the be-

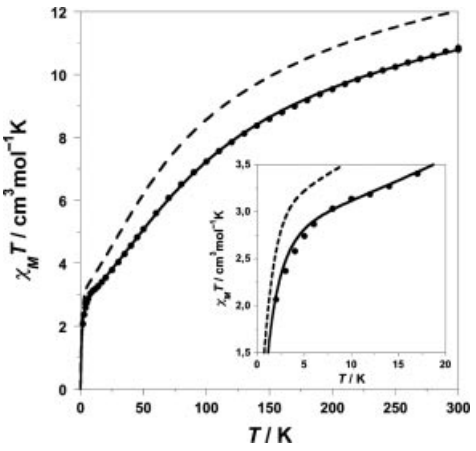

Figure 9. Magnetic susceptibility curves for **2** obtained from the calculated J values (dashed line) and fitted J values (solid line) that are shown in Table 6. The experimental data is displayed as black circles.

Table 6. Exchange coupling constants ($J_{i,j}$, cm^{-1}) obtained for **2** from theoretical calculations (A) and fitted values (B) in the temperature range 300–20 K. We also indicate the g factor, agreement factor (F), the spin ground state (GS) and the relative energy of first excited state (E_1, in cm^{-1}).

$J_{i,j}$	A	B
$J_{4,7}$	–52.7	–39.0
$J_{3,7}$	–3.8	+1.1
$J_{4,6}$	–2.8	+1.1
$J_{4,5}$	–26.2	–20.0
$J_{3,4}$	–25.7	–20.0
$J_{3,6}$	–10.6	–16.0
$J_{1,3}$	–4.8	–4.8
$J_{1,6}$	–3.9	–4.8
$J_{1,4}$	–1.4	–4.8
$J_{1,7}$	+0.8	–4.8
g factor	–	1.919
F	–	$5.1 \cdot 10^{-5}$
GS	0	0
E_1[a]	0.23 (1)	0.18 (1)

[a] S value of the first excited state in parentheses.

haviour observed for the dependence of the magnetisation with magnetic field at several temperatures. From an energy-level diagram obtained from calculated J values (Figure S5), we observe that some singlet, triplet, quintet and septet states are very close to the ground spin state. At slightly higher energy we can also find the first nonet state. Thus, when the applied magnetic field is increased some *ms* eigenfunctions of low-lying excited states with higher multiplicity will be populated reaching a non-zero-saturation value. In this situation the shape of the magnetisation curve and the saturation value are dependent on the temperature, because low-lying excited states will be populated at higher temperature. A similar behaviour is observed with the parameters obtained in the fit.

Conclusions

In conclusion, the reactions between $CrCl_2$ and the tripodal ligands H_3thme, H_3tmp, and H_4peol have produced new di- and octanuclear Cr^{III} clusters. Complex **1** can only be made under reflux and complexes **2** and **3** only under solvothermal conditions. Complexes **2** and **3** represent rare examples of "large" Cr clusters containing no bridging carboxylates with structures derived from the decametallate core commonly seen in polyoxometallate chemistry. As such, **1**–**3** may represent the first examples in a large family of Cr clusters and variations of the above reaction schemes may lead to the isolation of diverse metal polyhedra exhibiting novel magnetic properties. Magneto-structural correlations for $[Cr_2(OR)_2]^{4+}$ and $[Cr_2O_2]^{2+}$ complexes have been found, which we hope will help the analysis of the magnetic properties in new polynuclear Cr^{III} clusters. Electronic-structure calculations based on density functional theory have allowed us to understand the electronic factors that govern these correlations. Electronic structure calculations have been performed on **1** and **2** and good estimates of the J values have been obtained. Different sets of J values have been found to reproduce the magnetic behaviour of **2**. An analysis of the theoretical results and those obtained in the fitting procedure by diagonalisation of the Hamiltonian matrix allowed us to select one among the fitted J value sets.

Experimental Section

$[Cr_2(H_2tmp)_2Cl_4]\cdot 2MeOH$ (1·2MeOH): Anhydrous $CrCl_2$ (0.5 g, 4.0 mmol), H_3tmp (0.545 g, 4.0 mmol) and NaOMe (0.110 g, 2.0 mmol) were heated at reflux in MeOH (30 mL) for 3 h. The reaction mixture was filtered and the resulting dark green solution cooled. The solvent was then removed under reduced pressure and the resulting dark green solid recrystallised from MeCN (20 mL). Green crystals of **1** appeared upon Et_2O diffusion over 2 weeks. Yield based on Cr^{III}: 0.230 g (20%). $C_{14}H_{32}Cl_4Cr_2O_8$ (574.22): calcd. C 29.18, H 5.95; found C 28.99, H 5.85. IR (KBr pellet): $\tilde{\nu}$ = 3424 (s), 3170 (s), 2978 (s), 2604 (m), 1630 (w), 1453 (m), 1384 (m), 1299 (m), 1265 (w), 1189 (w), 1100 (s), 1040 (s), 940 (s), 773 (w), 592 (m), 560 (s), 509 (m), 443 (w) cm^{-1}. $[Cr_2(H_2tmp)_2Cl_4]\cdot$ 2MeOH (576.22): calcd. C 29.18, H 5.95; found: C 28.99, H 5.85.

$[Cr_8O_2(thme)_2(Hthme)_4Cl_6]\cdot 2MeOH$ (2·2MeOH): This complex was synthesised by heating $CrCl_2$ (0.3 g, 2.4 mmol), H_3thme (0.29 g, 2.4 mmol) and NaOMe (0.13 g, 2.4 mmol) in MeOH (9 mL) in a teflon-lined autoclave at 100 °C for 12 h. Slow cooling to room temperature yielded dark green crystals of **2**. Yield based on Cr^{III}: 0.130 g (30%). $C_{32}H_{62}Cl_6Cr_8O_{29}$ (1427.28): calcd. C 26.85, H 4.65; found C 26.28, H 4.67. IR (KBr pellet): 3420 (s), 2930 (s), 2361 (m), 1636 (w), 1464 (w), 1385 (w), 1124 (m), 1044 (s), 630 (m), 580 (s), 536 (m), 468 (w) cm^{-1}.

$[Cr_8O_2(Hpeol)_2(H_2peol)_4Cl_6]\cdot 3MeOH$ (3·3MeOH): The complex was synthesised as **2**, replacing H_3thme with H_4peol. $C_{33}H_{60}Cl_6Cr_8O_{22}$ (1549.27): calcd. C 25.31, H 4.89; found C 25.63, H 4.97. IR (KBr pellet): $\tilde{\nu}$ = 3450 (s), 2931 (m), 2874 (m), 1636 (w), 1472 (w), 1388 (w), 1224 (w), 1115 (s), 1060 (s), 653 (m), 593 (s), 537 (m), 506 cm^{-1} (w).

Table 7. Crystallographic data for complexes **1**–**3**.

	1 [Cr_2]	**2** [Cr_8thme]	**3** [Cr_8peol]
Formula	$C_{14}H_{34}Cl_4Cr_2O_8$	$C_{32}H_{66}Cl_6Cr_8O_{22}$	$C_{33}H_{70}Cl_6Cr_8O_{27}$
M [g·mol^{-1}]	576.12	1427.52	1565.62
Crystal system	monoclinic	triclinic	monoclinic
Space group	$P2_1/c$	$P\bar{1}$	$C2/c$
a [Å]	9.3936(32)	10.0553(19)	13.1762(6)
b, Å	10.0550(34),	10.968(2)	17.5288(8)
c [Å]	12.4914(42)	12.671(2)	22.9112(11)
α [°]	90	79.722(15)	90
β [°]	99.812(6)	67.844(18)	99.468(4)
γ [°]	90	89.221(15)	90
V [Å^3]	1162.6(7)	1271.3(4)	5219.6(4)
T [K]	100(2)	100(2)	100(2)
Z	2	2	4
$\rho_{calcd.}$ [g cm^{-3}]	1.646	1.870	1.985
Crystal shape and colour	green block	green block	green block
Crystal size [mm]	0.08 × 0.04 × 0.01	0.37× 0.20× 0.08	0.35× 0.24 × 0.13
μ [mm^{-1}]	1.430	2.032	1.998
Unique data	1676	7850	8477
Unique data, [$I > 2\,\theta\,(F)$]	1430	6443	6309
R_1, wR_2	0.0290, 0.0705	0.0572, 0.1572	0.0572, 0.1469
Goodness of fit	1.060	1.090	1.022

X-ray Crystallography: Data were collected with either Bruker SMART APEX CCD (1) or Oxford Diffraction Crysalis CCD diffractometers (**2**, **3**) at 100(2) K using Mo-K_α radiation (λ = 0.71073 Å). Both structures were solved by direct methods and refined (on F^2 for all reflections) using SHELXTL.[43,44] Absorption corrections were applied using SADABS (**1**) and software built into the Crysalis CCD program (**2**, **3**). All non-hydrogen atoms were refined anisotropically. Excessive thermal motion of the chlorine atoms in **1** required thermal and angular restraints to be applied. Neither refinement nor absorption corrections reduced the residual electron density in the core of **2**. The hydrogen atoms in **2** could not be found so were added in calculated positions. Relevant crystallographic information for the compounds is summarised in Table 7. CCDC-285702–285704 contain the supplementary crystallographic data for this paper. These data can be obtained free of charge from The Cambridge Crystallographic Data Centre via www.ccdc.cam.ac.uk/data_request/cif.

Magnetic Measurements: Variable-temperature, solid-state direct current (dc) magnetic susceptibility data down to 1.80 K were collected with a Quantum Design MPMS-XL SQUID magnetometer equipped with a 5.5-T dc magnet at the University of Barcelona. Diamagnetic corrections were applied to the observed paramagnetic susceptibilities using Pascal's constants.

Computational Details: All theoretical calculations were carried out with the hybrid B3LYP method,[45–47] as is implemented in the Gaussian03 program.[48] Double-ζ (SV) and triple-ζ (TZV) quality basis sets proposed by Ahlrichs and co-workers have been used for all atoms.[49,50] For the chromium ions, two extra p functions have been added. The electronic configurations used as starting points have been created using Jaguar 6.0 software. The broken-symmetry approach has been employed to describe the unrestricted solutions of the antiferromagnetic spin states.[51–53] No molecular modelling has been done, with the full experimental geometry of **2** used for the calculations. A quadratic convergence method was employed to determine the more stable wave functions in the SCF process.[54] The atomic spin densities were obtained from Natural Bond Orbital (NBO) analysis.[55–57]

Other Measurements: Elemental analyses were performed by the University of Manchester Microanalysis Service. IR spectra were recorded as KBr pellets on a Nicolet model 510P spectrophotometer.

Acknowledgments

This work was supported by the Lloyds of London Tercentenary Foundation (UK), EPSRC (UK), The Leverhulme Trust (UK), Dirección General de Enseñanza Superior (DGES) and Comissió Interdepartamental de Ciència i Tecnologia (CIRIT) through the grants CTQ2005-08123-C02-02/BQU and 2005SGR-00036, respectively. The computing resources were generously made available in the Centre de Computació de Catalunya (CESCA) with a grant provided by Fundació Catalana per a la Recerca (FCR) and the Universitat de Barcelona.

[1] E. J. L. McInnes, S. Piligkos, G. A. Timco, R. E. P. Winpenny, *Coord. Chem. Rev.* **2005**, *249*, 2577.
[2] R. H. Laye, E. J. L. McInnes, *Eur. J. Inorg. Chem.* **2004**, 2811.
[3] D. Collison, M. Murrie, V. S. Oganesyan, S. Piligkos, N. R. J. Poolton, G. Rajaraman, G. M. Smith, A. J. Thomson, G. A. Timko, W. Wernsdorfer, R. E. P. Winpenny, E. J. L. McInnes, *Inorg. Chem.* **2003**, *42*, 5293.
[4] A. Bino, D. C. Johnston, D. P. Goshorn, T. R. Halbert, E. I. Stiefel, *Science* **1988**, *241*, 1479.
[5] R. Basler, C. Boskovic, G. Chaboussant, H. U. Güdel, M. Murrie, S. T. Ochsenbein, A. Sieber, *ChemPhysChem* **2003**, *4*, 910.
[6] J. Telser, J. van Slageren, S. Vongtragool, M. Dressel, W. M. Reiff, S. A. Zvyagin, A. Ozarowski, J. Krzystek, *Magn. Reson. Chem.* **2005**, *43*, S130.
[7] S. Piligkos, G. Rajaraman, M. Soler, N. Kirchner, J. van Slageren, R. Bircher, S. Parsons, H. U. Güdel, J. Kortus, W. Wernsdorfer, G. Christou, E. K. Brechin, *J. Am. Chem. Soc.* **2005**, *127*, 5572.
[8] E. K. Brechin, *Chem. Commun.* **2005**, 5141.
[9] M. I. Khan, J. Zubieta, *Prog. Inorg. Chem.* **1995**, *43*, 1.
[10] K. G. Caulton, M. H. Chisholm, S. R. Drake, K. Folting, J. C. Huffman, *Inorg. Chem.* **1993**, *32*, 816.
[11] W. J. Evans, D. G. Giarikos, M. A. Greci, J. W. Ziller, *Eur. J. Inorg. Chem.* **2002**, 453.
[12] R. C. Finn, J. Zubieta, *J. Cluster Sci.* **2000**, *11*, 461.
[13] M. Cavaluzzo, Q. Chen, J. Zubieta, *J. Chem. Soc., Chem. Commun.* **1993**, 131.
[14] J. Cano, in *VPMAG, Revision C01*, Universitat de València, Valencia, **2004**.
[15] I. M. Atkinson, C. Benelli, M. Murrie, S. Parsons, R. E. P. Winpenny, *Chem. Commun.* **1999**, 285.
[16] F. E. Mabbs, E. J. L. McInnes, M. Murrie, S. Parsons, G. M. Smith, C. C. Wilson, R. E. P. Winpenny, *Chem. Commun.* **1999**, 643.
[17] S. Parsons, A. A. Smith, R. E. P. Winpenny, *Chem. Commun.* **2000**, 579.
[18] B. G. Gafford, R. E. Marsh, W. P. Schaefer, J. H. Zhang, C. J. Oconnor, R. A. Holwerda, *Inorg. Chem.* **1990**, *29*, 4652.
[19] B. G. Gafford, R. A. Holwerda, *Inorg. Chem.* **1990**, *29*, 4353.
[20] N. K. Dalley, X. L. Kou, C. J. O'Connor, R. A. Holwerda, *Inorg. Chem.* **1996**, *35*, 2196.
[21] M. Eshel, A. Bino, *Inorg. Chim. Acta* **2002**, *329*, 45.
[22] H. R. Fischer, J. Glerup, D. J. Hodgson, E. Pedersen, *Inorg. Chem.* **1982**, *21*, 3063.
[23] J. J. H. Edema, S. Gambarotta, W. J. J. Smeets, A. L. Spek, *Inorg. Chem.* **1991**, *30*, 1380.
[24] M. Divaira, F. Mani, *Inorg. Chem.* **1984**, *23*, 409.
[25] B. G. Gafford, R. A. Holwerda, H. J. Schugar, J. A. Potenza, *Inorg. Chem.* **1988**, *27*, 1126.
[26] F. Bottomley, D. E. Paez, L. Sutin, P. S. White, F. H. Kohler, R. C. Thompson, N. P. C. Westwood, *Organometallics* **1990**, *9*, 2443.
[27] F. Bottomley, D. E. Paez, P. S. White, *J. Am. Chem. Soc.* **1981**, *103*, 5581.
[28] F. Bottomley, D. E. Paez, P. S. White, *J. Am. Chem. Soc.* **1982**, *104*, 5651.
[29] N. J. Robertson, M. J. Carney, J. A. Halfen, *Inorg. Chem.* **2003**, *42*, 6876.
[30] K. B. P. Ruppa, K. Feghali, I. Kovacs, K. Aparna, S. Gambarotta, G. P. A. Yap, C. Bensimon, *J. Chem. Soc., Dalton Trans.* **1998**, 1595.
[31] D. J. Hodgson, in: *Magneto-Structural Correlations in Exchange Coupled Systems, Vol. 140* (Eds.: R. D. Willet, D. Gatteschi, O. Kahn), NATO ASI Series C, Dordrecht, **1985**, p. 497.
[32] E. Ruiz, P. Alemany, S. Alvarez, J. Cano, *Inorg. Chem.* **1997**, *36*, 3683.
[33] E. Ruiz, P. Alemany, S. Alvarez, J. Cano, *J. Am. Chem. Soc.* **1997**, *119*, 1297.
[34] E. D. Estes, R. P. Scaringe, W. E. Hatfield, D. J. Hodgson, *Inorg. Chem.* **1976**, *15*, 1179.
[35] E. D. Estes, R. P. Scaringe, W. E. Hatfield, D. J. Hodgson, *Inorg. Chem.* **1977**, *16*, 1605.
[36] D. A. House, V. McKee, P. J. Steel, *Inorg. Chem.* **1986**, *25*, 4884.
[37] W. Clegg, *Acta Crystallogr., Sect. C* **1985**, *41*, 1830.
[38] H. R. Fischer, D. J. Hodgson, E. Pedersen, *Inorg. Chem.* **1984**, *23*, 4755.

[39] R. Clerac, F. A. Cotton, C. A. Murillo, X. P. Wang, *Chem. Commun.* **2001**, 205.
[40] T. K. Paine, T. Weyhermuller, K. Wieghardt, P. Chaudhuri, *Inorg. Chem.* **2002**, *41*, 6538.
[41] M. V. Barybin, P. L. Diaconescu, C. C. Cummins, *Inorg. Chem.* **2001**, *40*, 2892.
[42] R. Carrasco, J. Cano, T. Mallah, L. F. Jones, D. Collison, E. K. Brechin, *Inorg. Chem.* **2004**, *43*, 5410.
[43] G. M. Sheldrick, in *SHELXL-97*, University of Gottingen, Germany, **1997**.
[44] P. T. Beurskens, G. Beurskens, W. P. Bosman, R. de Gelder, S. Garcia-Granada, R. O. Gould, R. Israel, J. M. M. Smits, in *DIRDIF96 Program System*, Technical Report of the Crystallography Laboratory, University of Nijmegen, The Netherlands, **1996**.
[45] A. D. Becke, *Phys. Rev. A* **1988**, *38*, 3098.
[46] C. T. Lee, W. T. Yang, R. G. Parr, *Phys. Rev. B* **1988**, *37*, 785.
[47] A. D. Becke, *J. Chem. Phys.* **1993**, *98*, 5648.
[48] M. J. Frisch, G. W. Trucks, H. B. Schlegel, G. E. Scuseria, M. A. Robb, J. R. Cheeseman, J. Montgomery, J. A., T. Vreven, K. N. Kudin, J. C. Burant, J. M. Millam, S. S. Iyengar, J. Tomasi, V. Barone, B. Mennucci, M. Cossi, G. Scalmani, N. Rega, G. A. Petersson, H. Nakatsuji, M. Hada, M. Ehara, K. Toyota, R. Fukuda, J. Hasegawa, M. Ishida, T. Nakajima, Y. Honda, O. Kitao, H. Nakai, M. Klene, X. Li, J. E. Knox, H. P. Hratchian, J. B. Cross, V. Bakken, C. Adamo, J. Jaramillo, R. Gomperts, R. E. Stratmann, O. Yazyev, A. J. Austin, R. Cammi, C. Pomelli, J. W. Ochterski, P. Y. Ayala, K. Morokuma, G. A. Voth, P. Salvador, J. J. Dannenberg, V. G. Zakrzewski, S. Dapprich, A. D. Daniels, M. C. Strain, O. Farkas, D. K. Malick, A. D. Rabuck, K. Raghavachari, J. B. Foresman, J. V. Ortiz, Q. Cui, A. G. Baboul, S. Clifford, J. Cioslowski, B. B. Stefanov, G. Liu, A. Liashenko, P. Piskorz, I. Komaromi, R. L. Martin, D. J. Fox, T. Keith, M. A. Al-Laham, C. Y. Peng, A. Nanayakkara, M. Challacombe, P. M. W. Gill, B. Johnson, W. Chen, M. W. Wong, C. Gonzalez, J. A. Pople, in *Gaussian 03, Revision C.02*, Gaussian 03, Revision C.02 ed., Gaussian, Inc. Wallingford CT, **2004**.
[49] A. Schäfer, H. Horn, R. Ahlrichs, *J. Chem. Phys.* **1992**, *97*, 2571.
[50] A. Schäfer, C. Huber, R. Ahlrichs, *J. Chem. Phys.* **1994**, *100*, 5829.
[51] E. Ruiz, J. Cano, S. Alvarez, P. Alemany, *J. Comput. Chem.* **1999**, *20*, 1391.
[52] E. Ruiz, S. Alvarez, A. Rodríguez-Fortea, P. Alemany, Y. Puoillon, C. Massobrio, in: *Magnetism: Molecules to Materials, Vol. II* (Eds.: J. S. Miller, M. Drillon), Wiley-VCH, Weinheim, **2001**, pp. 5572.
[53] E. Ruiz, A. Rodriguez-Fortea, J. Cano, S. Alvarez, P. Alemany, *J. Comput. Chem.* **2003**, *24*, 982.
[54] G. B. Bacskay, *Chem. Phys.* **1981**, *61*, 385.
[55] J. E. Carpenter, F. Weinhold, *J. Mol. Struct. (Theochem)* **1988**, *169*, 41.
[56] A. E. Reed, L. A. Curtiss, F. Weinhold, *Chem. Rev.* **1988**, *88*, 899.
[57] F. Weinhold, J. E. Carpenter, *The Structure of Small Molecules and Ions*, Plenum, **1988**.
[58] F. H. Allen, O. Kennard, *Chem. Des. Autom. News* **1993**, *8*, 31.
Received: May 24, 2006
Published Online: July 11, 2006

